

1 **Identification of nitrogen-dependent QTL and underlying genes** 2 **for root system architecture in hexaploid wheat**

3 Marcus Griffiths¹, Jonathan A. Atkinson¹, Laura-Jayne Gardiner², Ranjan Swarup¹, Michael P.
4 Pound³, Michael H. Wilson¹, Malcolm J. Bennett¹ & Darren M. Wells^{1*}.

5 ¹School of Biosciences, University of Nottingham, Loughborough, LE12 5RD, UK.

6 ²IBM Research, Warrington, WA4 4AD, UK.

7 ³School of Computer Science, University of Nottingham, Nottingham, NG8 1BB, UK.

8

9 *Correspondence to D.M.W.

10 e-mail: darren.wells@nottingham.ac.uk

11

12 Date of submission – 27 March 2019

13 No. words in summary – 199

14 No. words in main text – 3574

15 No. words in introduction – 490

16 No. words in Materials and Methods – 1043

17 No. words in Results – 1158

18 No. words in Discussion – 793

19

20 No. tables – 4

21 No. figures – 6 (all colour print)

22 Supplementary Data – 3 x Supplementary Tables, 1 x Supplementary Figure

23

24 M. Griffiths: mdgriffiths@noble.org ORCID iD: 0000-0003-2349-8967

25 J. A. Atkinson: jonathan.atkinson@nottingham.ac.uk ORCID iD: 0000-0003-2815-0812

26 L. J. Gardiner: laura-jayne.gardiner@ibm.com ORCID iD: 0000-0002-9177-4452

27 R. Swarup: ranjan.swarup@nottingham.ac.uk ORCID iD: 0000-0002-6438-9188

28 M. P. Pound: michael.pound@nottingham.ac.uk ORCID iD: 0000-0002-5016-1078

29 M. H. Wilson: michael.wilson@nottingham.ac.uk ORCID iD: 0000-0002-6323-6059

30 M. J. Bennett: malcolm.bennett@nottingham.ac.uk ORCID iD: 0000-0003-0475-390X

31 D. M. Wells: darren.wells@nottingham.ac.uk Tel. +44 115 951 6373 ORCID iD: 0000-0002-
32 4246-4909

56 **Abbreviations**

57 ABA, Abscisic acid; BLUEs, best linear unbiased estimates; BLUPS, best linear unbiased
58 predictions; DAG, days after germination; DH, doubled haploid; LOD, logarithm of odds;
59 nabim, National Association of British & Irish Millers; NPF, peptide transporter family; NRT,
60 nitrate transporter; NUE; nitrogen use efficiency; PTR, proton-dependent oligopeptide
61 transporter; QTL, quantitative trait locus; RNA-seq, RNA sequencing technology; RSA, root
62 system architecture; RSML, Root System Markup Language.

63 **Introduction**

64 Nitrogen (N) is an essential macronutrient for plant growth and development with agriculture
65 greatly dependent on synthetic N fertilisers for enhancing productivity. Global demand for
66 fertilisers is projected to rise by 1.5% each year reaching 201.7 million tonnes in 2020, over
67 half of which (118.8 million tonnes) is for nitrate fertilizers (FAO, 2017). However, there are
68 compelling economic and environmental reasons to reduce N fertiliser use in agriculture,
69 particularly as the N fixing process is reliant on unsustainable fossil fuels (Dawson *et al.*, 2008).

70

71 The availability of nutrients is spatially and temporally heterogeneous in the soil. Roots
72 therefore need to forage for such resources. The spatial arrangement of the root system, called
73 the root system architecture (RSA) (Hodge *et al.*, 2009), has a profound effect on the uptake of
74 nutrients and consequently the potential yield. Optimisation of the RSA could significantly
75 improve the efficiency of resource acquisition and in turn increase the yield potential of the
76 crop. An improvement in N use efficiency (NUE) by just 1% could reduce fertiliser losses and
77 save ~\$1.1 billion annually (Delogu *et al.*, 1998; Kant *et al.*, 2010).

78 Understanding the contribution of root traits to RSA and function is of central importance for
79 improving crop productivity. Roots however are inherently challenging to study leading to the
80 wide use of artificial growth systems for plant phenotyping as they are generally high-
81 throughput, allow precise control of environmental parameters and are easy to replicate. These
82 phenotyping systems have been key for generating root phenotypic data for association
83 mapping and uncovering underlying genetic mechanisms (Ren *et al.*, 2012; Clark *et al.*, 2013;
84 Atkinson *et al.*, 2015; Zurek *et al.*, 2015). For cereals, understanding the genetic basis of RSA
85 is complex due to the polyploid nature and large genome sizes. Therefore, quantitative trait loci
86 (QTL) analyses have been very useful for precisely linking phenotypes to regions of a
87 chromosome. With the development of high-throughput RNA sequencing technology (RNA-
88 seq), identified QTL can now be further dissected to the gene level. Using RNA-seq, a
89 substantial number of genes and novel transcripts have been identified in cereal crops including
90 rice, sorghum, maize and wheat that are implicated in RSA control (Oono *et al.*, 2013; Gelli *et al.*
91 *et al.*, 2014; Akpinar *et al.*, 2015; Yu *et al.*, 2015). To our knowledge, there are no other studies
92 that have identified genes related to nitrate response or root angle change in wheat. The
93 uncovering of these genes and mechanisms are likely to be of agronomical importance as they

94 can then be implemented in genomics-assisted breeding programs to improve N-uptake
95 efficiency in crops.

96 The aim of this study was to identify root traits and genes that relate to N uptake and plasticity
97 in wheat. To achieve this, a germination paper-based system was used to phenotype a wheat
98 doubled haploid (DH) mapping population under two N regimes. Here were present genomic
99 regions and underlying genes that we propose may control an N-dependent root angle response
100 in wheat.

101 **Materials and methods**

102 *Plant materials*

103 A winter wheat doubled haploid mapping population comprised of 94 lines was used for root
104 phenotyping. The population was derived from a cross between cultivars Savannah and Rialto
105 F1 plants (Limagrain UK Ltd, Rothwell, UK). Both parents are UK winter wheat cultivars that
106 were on the AHDB recommended list. Savannah is a National Association of British & Irish
107 Millers (nabim) Group 4 feed cultivar first released in 1998. Rialto is nabim Group 2 bread-
108 making cultivar first released in 1995.

109 *Seedling phenotyping*

110 Wheat seedlings were grown hydroponically using the system described in Atkinson *et al.*
111 (2015) (Fig. 1). Seeds from the Savannah × Rialto doubled haploid (S×R DH) mapping
112 population were sieved to a seed size range of 2.8–3.35 mm based on mean parental seed size.
113 Seeds were surface sterilised in 5% (v/v) sodium hypochlorite for 12 minutes before three
114 washes in dH₂O. Sterilised seeds were laid on wet germination paper (Anchor Paper Company,
115 St Paul, MN, USA) and stratified at 4°C in a dark controlled environment room for 5 days.
116 After stratification seeds were transferred to a controlled environment room at 20/15°C, 12
117 hour photoperiod, 400 $\mu\text{mol m}^{-2} \text{s}^{-1}$ PAR and kept in a light-tight container. After 48 hours,
118 uniformly germinated seedlings with ~5 mm radicle length were transferred to vertically
119 orientated seedling pouches.

120

121 Seeds for 94 lines from the S×R DH mapping population were grown hydroponically either in
122 high N (3.13 mM NO₃⁻) or low N (0.23 mM NO₃⁻) modified Hoagland's solution (Table S1).
123 The experimental design was a randomised block comprised of 94 genotypes split over 11
124 experimental runs with a target of 20 replications per genotype ($n = 8 - 36$). The root system
125 architecture of each seedling was extracted from the images and stored in Root System Markup
126 Language (RSML, Lobet *et al.*, 2015) using the root tracing software RootNav (Pound *et al.*,
127 2013). Root traits were quantified using RootNav standard functions and additional
128 measurements as described in Atkinson *et al.* (2015). The shoot length and area were extracted

129 from the shoot images using custom macros in the FIJI software package (Schindelin *et al.*,
130 2012). Definitions for all extracted traits are in Table 1.

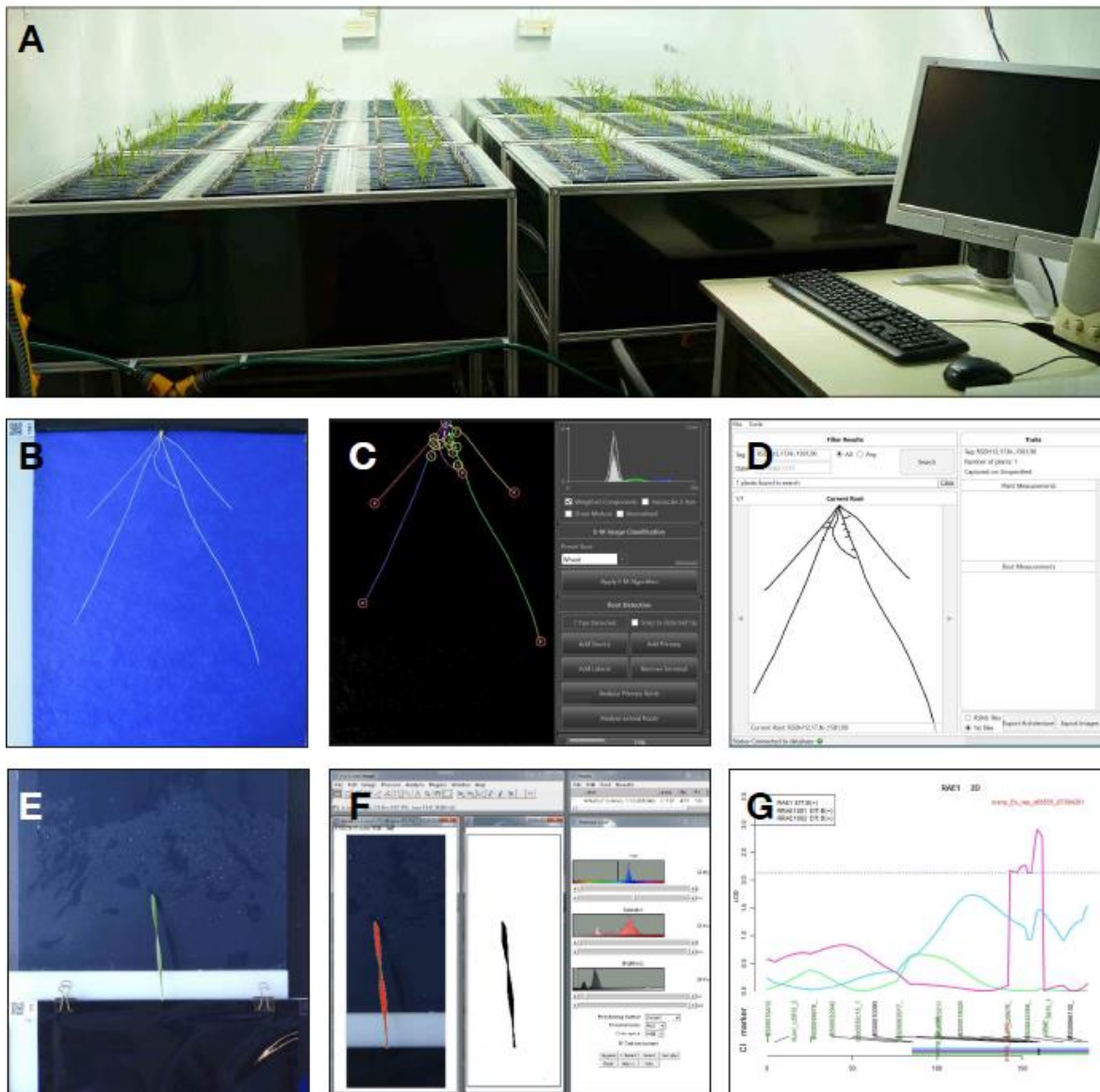


Fig. 1. High-throughput hydroponic phenotyping system for seedling root & shoot traits. (a) Growth assembly and plant imaging station. (b) Example image of a wheat root grown on germination paper 10 DAG. (c) Root system extraction to RSML database using RootNav software. (d) Measurement of root traits from RSML database. (e) Example image of a wheat shoot 10 DAG. (f) Shoot image colour thresholding & shoot measurement using FIJI. (g) Example of QTL peak extracted from phenotyping data & mapping data with rQTL.

131 *Quantitative trait locus mapping*

132 Detection of QTL was conducted using the R Statistics package “R/qtl” (Broman *et al.*, 2003).
133 The map used was a high-density Savannah × Rialto iSelect map obtained from Wang *et al.*
134 (2013) with redundant and closer than 0.5 cM markers stripped out. Before data processing,
135 the best linear unbiased estimates (BLUEs) or best linear unbiased predictions (BLUPs) were
136 calculated for the traits if necessary. QTL were identified based on the extended Haley-Knott
137 algorithm (Haley & Knott, 1992). The threshold logarithm of the odds (LOD) scores were
138 calculated by 1000 × permutation test at $p < 0.05$ level (Churchill & Doerge, 1994). The
139 threshold for declaring presence of a QTL was a LOD score of 2.0. The annotated linkage map
140 was generated using R Statistics package “LinkageMapView” (Ouellette *et al.*, 2018).

141 *RNA-sequencing of candidate QTL*

142 RNA-seq was used to identify underlying genes for a candidate QTL with expression levels
143 changed by N treatment. Pooled root samples were immediately frozen after collection using
144 liquid nitrogen and stored at -80°C . The sample groups, +QTL/-QTL, each consisted of four
145 biological replicate pools where each pool was made up of four independent lines (4x3 plants
146 per line). Total RNA was isolated from 500–1000 mg of homogenised root tissue (TRIzol
147 reagent). RNA quality and purity was determined using a NanoDropTM 2000c with values
148 above $500 \text{ ng } \mu\text{L}^{-1}$ or higher accepted. Illumina Paired-End Multiplexed RNA sequencing was
149 performed by Source Bioscience (Nottingham, UK).

150

151 Differential gene expression analysis was conducted using the IWGSC RefSeq v1.1 assembly
152 (International Wheat Genome Sequencing Consortium, 2018)
153 (http://plants.ensembl.org/Triticum_aestivum/) and the TGAC v1 Chinese Spring reference
154 sequence (Clavijo *et al.*, 2017). Raw sequencing reads were trimmed for adapter sequence and
155 for regions where the average quality per base dropped below 15 (Trimmomatic version 0.32)
156 (Bolger *et al.*, 2014). After trimming, reads below 40 bp were eliminated from the dataset.
157 Trimmed reads were aligned to the reference sequences assembly using splice-aware aligner
158 HISAT2 (Pertea *et al.*, 2016). Uniquely mapped reads were selected, and duplicate reads
159 filtered out. Unmapped reads across all samples were assembled into transcripts using
160 MaSuRCA software and sequences 250 bp or larger taken forward (Zimin *et al.*, 2013).
161 Unmapped reads were re-aligned to these assembled transcripts individually and added to their
162 sample specific reads while the assembled transcripts were combined with the reference

163 sequence and GTF annotation for downstream investigations. StringTie software was used to
164 calculate gene and transcript abundances for each sample across the analysis specific annotated
165 genes (Pertea *et al.*, 2016). Finally, DEseq was used to visualise results and identify differential
166 expression between samples (Anders & Huber, 2010). Differentially expressed genes were
167 compared between the IWGSC RefSeq v1.1 and TGAC v1 reference assemblies to identify
168 overlap using BLAST (BLASTN, e-value 1e-05, identity 95%, minimum length 40bp)
169 (Altschul *et al.*, 1990). The top matches for each gene between the reference sequences were
170 used to allow an integrative and comprehensive annotation of genes. Gene ontology (GO)
171 analysis was performed using the latest genome for *T. aestivum*. (IWGSC RefSeq v1.1
172 assembly) in g:Profiler (Reimand *et al.*, 2016).

173 *Phylogenetic analysis*

174 A phylogenetic analysis of protein families was conducted to compare the protein sequences
175 of *A. thaliana*, *O. sativa* L. and *T. aestivum* L. proton-dependent oligopeptide transporter (NPF)
176 families (also known as the NRT1/PTR family). *A. thaliana* sequences were obtained from
177 (Léran *et al.*, 2014). Using the latest genome for *T. aestivum*. (IWGSC RefSeq v1.1 assembly)
178 and *O. sativa*. (MSU Release 7.0, Kawahara *et al.*, 2013, <https://phytozome.jgi.doe.gov/>) a
179 HMM profile search was conducted (Krogh *et al.*, 2001). The resulting list of proteins were
180 scanned using Pfam (El-Gebali *et al.*, 2019). Only single gene models of candidate genes with
181 PTR2 domains were retained. The protein sequences were used to generate a maximum-
182 likelihood tree using the software RAxML (Stamatakis, 2014). The exported tree file (.NWK)
183 was then visualised using the R package “ggtree” (Yu *et al.*, 2017) and used for phylogenetic
184 tree construction. The exported tree file (.NWK) was visualised using the R package “ggtree”
185 (Yu *et al.*, 2017).

186 **Results**

187 *High-throughput hydroponic based system for phenotyping a wheat doubled haploid*
188 *population*

189 Seedlings for 92 lines of the S×R DH mapping population and parents were grown
190 hydroponically in a controlled environment chamber under high and low N treatments (Fig. 1).
191 Roots and shoots of each seedling were individually imaged 10 days after germination (DAG)
192 resulting in 6924 images. The phenotypic trait values for the parental lines, Savannah and
193 Rialto, under two N regimes are summarised in Table 2. Significant differences between the
194 parents were observed in root traits only with no significant shoot length or shoot area
195 differences ($p = ns$). For the root traits measured, differential responses to N treatment were
196 also observed. For all root length and size traits (except for lateral root length under low N)
197 Savannah was significantly larger ($p < 0.05$) than Rialto under both high and low N treatments.
198 There was no significant effect of N supply on root traits in Rialto except for a reduction in
199 seminal root count. Savannah, however, showed significant reduction in lateral root length,
200 convex hull area and maximum root depth under low N. There were no significant root angle
201 differences between the parents or N treatments, however lines within the DH population
202 showed transgressive segregation with trait values more extreme than the parents (Fig. 4, Table
203 2).

204 *Wheat root phenotypic traits segregate into two distinct clusters by size and angle*

205 A principal component analysis (PCA) was conducted to explore relationships within the root
206 phenotypic traits (Fig. 2a). Over 90% of the trait variation could be explained by the first six
207 principal components. There was no distinct grouping of lines based on the PCA phenotypic
208 relatedness. The loadings were mostly split between root size related traits and root angle and
209 distribution traits. An independent treatment effect was detected which opposed the root angle
210 loadings. A correlation matrix averaged between N treatments also demonstrated the strong
211 correlation between root size related traits and root angle and distribution related traits (Fig.
212 2b). In addition, the correlation analysis also highlighted negative associations between root
213 size and angle traits.

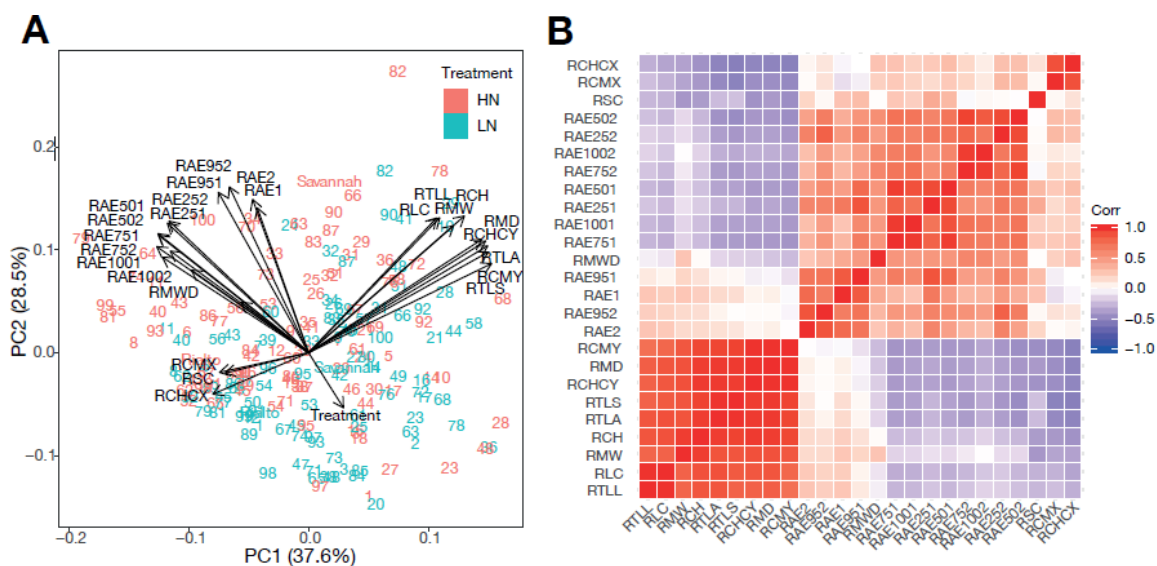


Fig. 2. (a) PCA ordination results for $S \times R$ doubled haploid population and parents under two N regimes. Black arrows indicate directions of loadings for each trait. (b) Correlation matrix of extracted root traits averaged between N treatments. Correlations are colour coded from strong positive correlation in red to strong negative correlation in blue with no correlation shown in white.

214 Identification of novel N-dependent root QTLs in the $S \times R$ DH population

215 A total of 55 QTLs were discovered for seedling root traits across both N treatments (Fig. 3,
216 Table 3), of which 36 came from Savannah, and 19 from Rialto. QTLs were found on
217 chromosomes 1A, 1B, 2D, 3B, 4D, 6D, 7A and 7D, with 23 QTLs located on 6D. Twenty-three
218 QTLs were identified under the low N treatment and 32 for the high N treatment. Nine QTLs
219 were found to be only present in the low N treatment, 18 QTLs were found only in the high N
220 treatment and 14 QTLs (28 total) were present in both N treatments. Phenotypic variation
221 explained by QTLs varied from 3.8 to 82.9%. Of the QTLs found, root size and vigour N

222 treatment independent QTLs were identified on chromosomes 6D and 7D. N-dependent QTLs
 223 were also found on chromosomes 6D and 7D that co-localised with other N independent root
 224 size QTLs. For N-dependent QTLs, root size QTLs were found on chromosomes 1A, 6D and
 225 7D. In addition, N-dependent root angle QTLs (RAE1001/751, LOD 3.0/2.6 respectively) were
 226 identified on chromosomes 2D, 3B and 4D. Of these regions a candidate N-dependent root
 227 angle QTL (RAE1001) residing on chromosome 2D was taken forward as it had the smallest
 228 peak confidence region (25 cM) for an N-dependent QTL (Table 4).

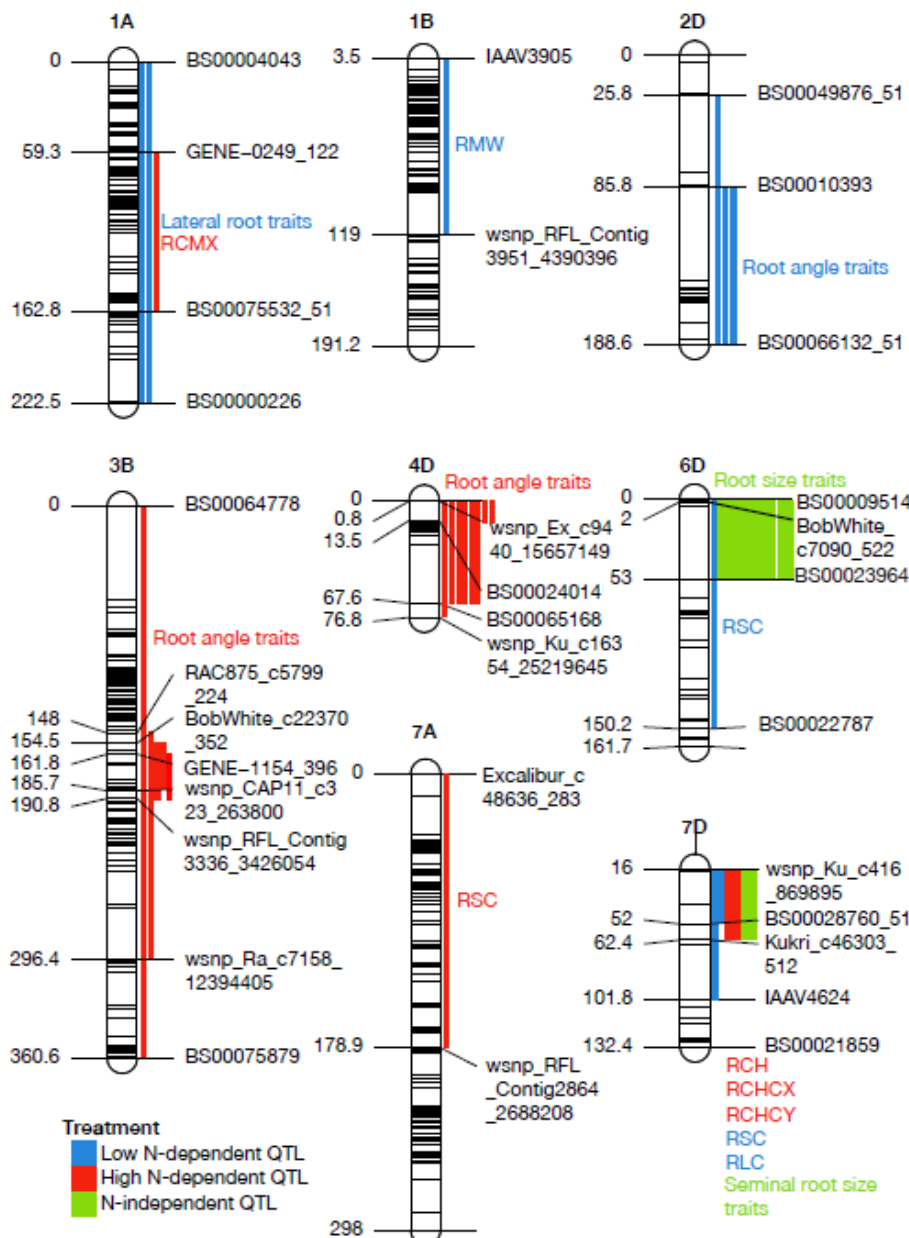


Fig. 3. Molecular linkage map showing position of QTLs detected in the S×R DH population grown in hydroponics. QTLs and confidence regions for all root traits are colour labelled for low N-dependent (blue), high N-dependent (red) and N treatment independent (green) (LOD > 2.0).

229 *Differentially regulated candidate genes on N-dependent root angle QTL identified by*
 230 *RNA-seq analysis*

231 The lines selected for the RNA-seq analysis were based on largest phenotypic differences for
 232 trait associated for a candidate N-dependent root angle QTL (RAE1001). Under low N there
 233 was a 30° difference in root angle between the extremes of the population with four lines of
 234 each taken forward for RNA-seq (Fig. 4a,b).

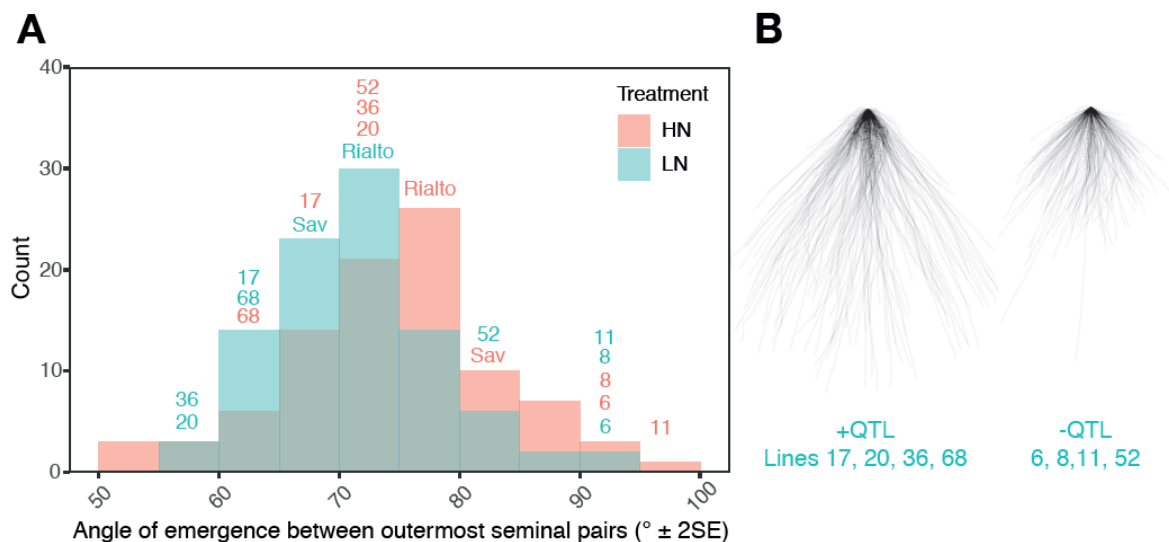


Fig. 4. (a) Distribution of means for seminal root angle (RAE1001) for S×R doubled haploid population under two N regimes. Labeled lines in blue were selected for RNA-seq. (b) Overlay plot for lines selected for RNA-seq that were the extremes of the population with differential seminal root angle (RAE1001).

235
 236 One sample group was comprised of lines that had the candidate QTL (Group A) and the second
 237 sample group did not have the QTL (Group B). As there was no single clear enriched region
 238 from the QTL analyses for the trait, the whole chromosome was considered for analysis. A
 239 total of 3299 differentially expressed genes were identified in the analysed groups. 1857
 240 differentially expressed genes showed significant ($p < 0.05$) up-regulation in Group A (with
 241 the QTL) compared to Group B (without QTL). Of these, 88 gene candidates resided on
 242 chromosome 2D. Additionally, MaSuRcA transcript assemblies were considered that were
 243 identified as significantly ($p < 0.05$) up-regulated in Group A compared Group B on
 244 chromosome 2D bringing the total to 93 (88 plus five) differentially expressed candidate
 245 sequences (Table S2). The inclusion of these *de novo* assembled transcript sequences in the
 246 analysis factors for varietal specific genes responsible for this phenotype that are not present

247 in the Chinese Spring based reference sequences. Of the 93 differentially expressed candidate
 248 sequences, 17 candidate genes were consistently expressed across the Group A replicates
 249 verses zero reads mapping in one or more Group B replicates and were therefore considered as
 250 our primary candidates (Table 4). There were also 1442 differentially expressed genes that
 251 showed significant ($p < 0.05$) down-regulation in Group A (with the QTL) compared to Group
 252 B (without QTL). Of these, 65 were annotated as residing on chromosome 2D (Table S2).

253
 254 Functional categories for the significantly up- and down-regulated genes were evaluated using
 255 g:profiler between the sample groups with and without N-dependent root QTL. For terms
 256 relating to biological processes there were 58 up-regulated terms that had the same lowest p-
 257 value including "nitrogen compound metabolic process", "cellular nitrogen compound
 258 metabolic process", "regulation of nitrogen compound metabolic process" and "cellular
 259 nitrogen compound biosynthetic process" (Fig. 5). For the down-regulated terms, three of the
 260 top 10 terms included "nitrogen compound metabolic process", "organonitrogen compound
 261 metabolic process" and "cellular nitrogen compound metabolic process" (Fig. 5). The complete
 262 list of enriched GO terms for molecular function, biological process and cellular component
 263 are available in Table S3.

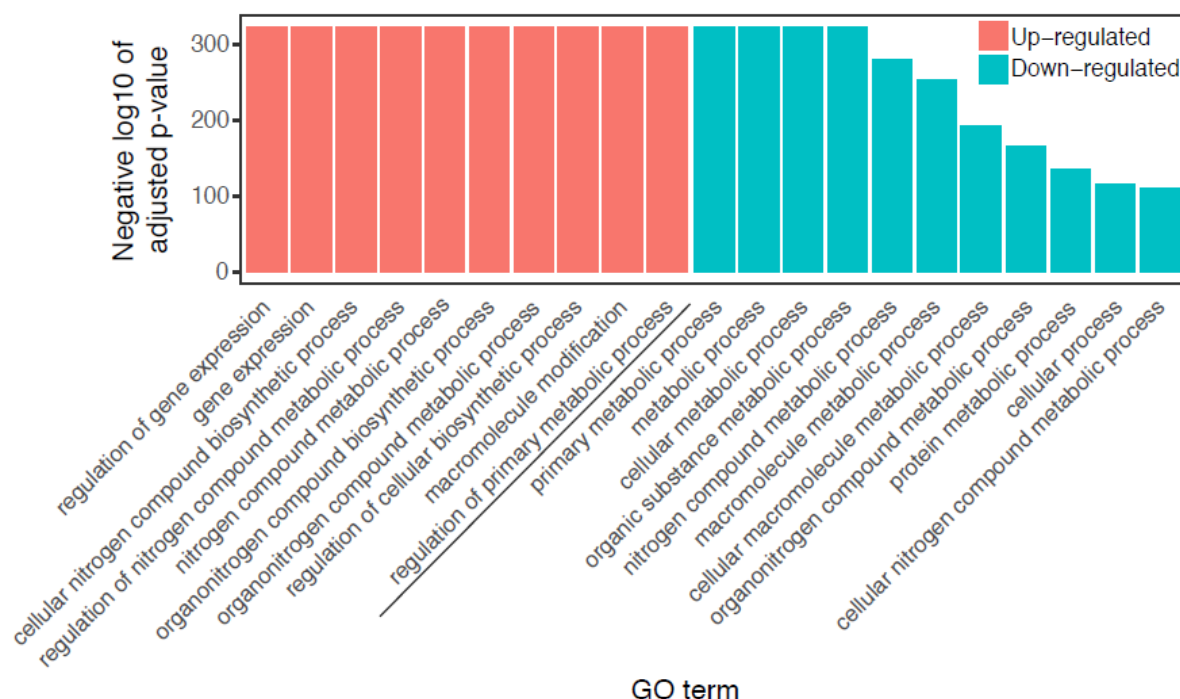


Fig. 5. GO enrichment analysis for top Biological process GO terms with the highest p-value for up- and down-regulated genes in the sample group with a candidate seminal root angle QTL compared to without the QTL.

264 *Putative nitrate uptake transporter involved with root angle change in wheat*

265 For the candidate N-dependent root angle QTL (RAE1001) there were a number of N-related
266 biological processes up- and down-regulated between the sample groups. In addition, within
267 the candidate gene list an up-regulated NPF family gene, TraesCS2D02G348400, was
268 identified which was consistently expressed across Group A and zero reads mapping in Group
269 B. Therefore, the function of this gene was pursued. A phylogenetic analysis of protein families
270 was conducted comparing NPF family protein sequences of *A. thaliana*, *O. sativa*. and *T.*
271 *aestivum* (Fig. S1). A total of 53 *A. thaliana* proteins, 130 *O. sativa*. proteins and 391 *T.*
272 *aestivum*. proteins were aligned using MUSCLE with 1000 bootstrap interactions and 20
273 maximum likelihood searches (Edgar, 2004). The candidate *T. aestivum*. protein
274 TraesCS2D02G348400 is situated in a monocot specific sub-clade within the NPF4 clade (Fig.
275 6). This clade includes *A. thaliana* NPF members AtNPF4.1, AtNPF4.2, AtNPF4.3, AtNPF4.4,
276 AtNPF4.5, AtNPF4.6 and AtNPF4.7. In addition, the candidate protein is closely related to a
277 rice nitrate(chlorate)/proton symporter protein LOC_Os04g41410.

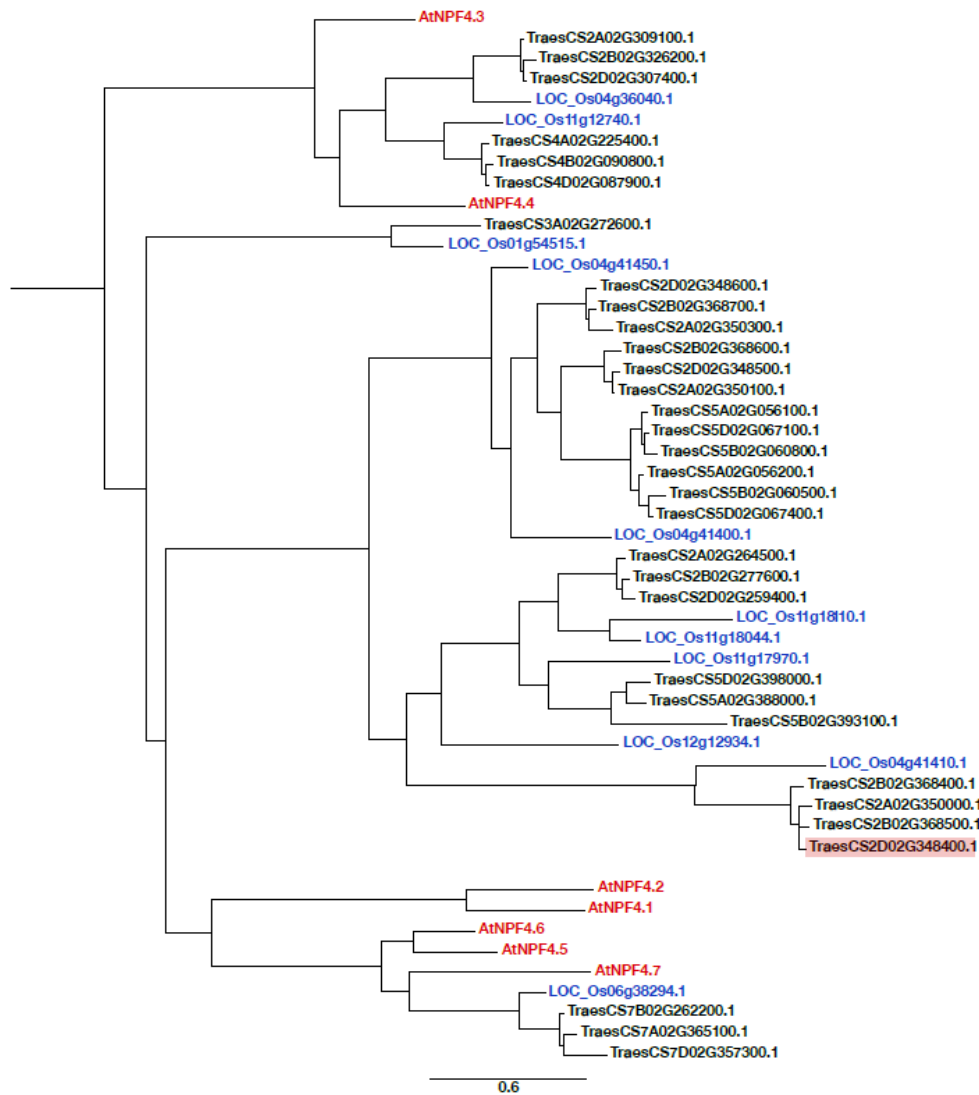


Fig. 6. Phylogenetic tree of protein families comparing the protein sequences of *A. thaliana*, *O. sativa* L. and *T. aestivum* L. NPF family proteins to an identified candidate *T. aestivum*. protein. The candidate *T. aestivum*. protein is situated in a monocot specific outgroup within a NPF4 protein clade (highlighted in red). Branch lengths are proportional to substitution rate.

278 Discussion

279 In this study, a total of 55 QTLs were discovered for seedling root traits across both N
 280 treatments (LOD > 2.0) (Fig. 3, Table 3). Of these loci, nine root QTLs were only detected in
 281 the low N treatment, 18 QTLs were found only in the high N treatment and 14 QTLs (28 total)
 282 were present in both N treatments.

283

284 In the literature, there are previously described QTL regions associated with architectural root
285 traits. On chromosome 1A QTL were found in this study for lateral root traits under low N
286 conditions. Interestingly chromosome 1A has been previously associated with lateral root
287 length in wheat and rice (Ren *et al.*, 2012; Beyer *et al.*, 2018). It appears that there are
288 underlying genes on chromosome 1A related to plasticity, tolerance and/or lateral root
289 development (An *et al.*, 2006; Landjeva *et al.*, 2008; Ren *et al.*, 2012; Guo *et al.*, 2012; Zhang
290 *et al.*, 2013; Liu *et al.*, 2013; Sun *et al.*, 2013). This region has also been correlated to NUp in
291 S×R field trials (Atkinson *et al.*, 2015) which would make the chromosome region an important
292 candidate for further study. On chromosomes 2D, 3B and 4D, N-dependent root angle QTLs
293 were identified in wheat grown in hydroponics. QTLs on these chromosomes have been
294 described in other studies but very few of these have measured root angle or distribution traits.
295 From comparison with other studies that found root QTLs on chromosome 2D it appears there
296 is an underlying gene for seminal root development and/or plasticity (An *et al.*, 2006; Zhang
297 *et al.*, 2013; Liu *et al.*, 2013). For chromosome 3B, other studies have found QTLs affecting
298 root size and stress related traits or genes relating to N plasticity, uptake or mobilisation (An *et*
299 *al.*, 2006; Habash *et al.*, 2007; Guo *et al.*, 2012; Zhang *et al.*, 2013; Bai *et al.*, 2013). For
300 chromosome 4D, comparing with other studies that found QTLs on this chromosome there
301 appears to be an underlying root development and/or root plasticity gene (Zhang *et al.*, 2013;
302 Bai *et al.*, 2013).

303

304 A low N-dependent seminal root angle QTL (LOD 3.0) on chromosome 2D was targeted for
305 transcriptomic analysis. A total of 17 candidate up-regulated genes were identified that were
306 up-regulated in this region (Table 4). A more detailed list of the genes identified are given in
307 Fig. S1. Two of the three genes with highest log changes plus four others have unknown
308 function. Point mutation detection and mutant generation with TILLING or RNAi represent
309 the next step to functionally characterise these genes.

310

311 A promising candidate from root transcriptomic analyses was a nitrate transporter 1/peptide
312 transporter (NPF) family gene, NPF4 (TraesCS2D02G348400). This gene was up-regulated in
313 an N-dependent manner related to a root angle QTL. Many N-related biological processes were
314 also up-regulated in the group of lines with the QTL. In *A. thaliana* and *O. sativa.*, NPF family
315 genes have important roles in lateral root initiation, branching and response to nitrate (Remans
316 *et al.*, 2006; Krouk *et al.*, 2010; Fang *et al.*, 2013). However, no studies have reported genes
317 controlling root angle change in wheat, to date. A phylogenetic analysis of protein families was

318 conducted comparing the protein sequences of *A. thaliana*, *O. sativa*. and *T. aestivum*. to the
319 candidate protein. The candidate *T. aestivum*. protein is situated in a monocot specific sub-
320 clade within the NPF4 clade and is closely related to a rice nitrate(chlorate)/proton symporter
321 protein (LOC_Os04g41410) (Fig. 6). Members of this clade are known for transporting the
322 plant hormone abscisic acid (ABA) (AtNPF4.1 and AtNPF4.6) and have been demonstrated to
323 have low affinity nitrate transport activity (AtNPF4.6) (Huang *et al.*, 1999; Kanno *et al.*, 2012).
324 ABA is known to be a key regulator in root hydrotropism, a process that senses and drives
325 differential growth towards preferential water potential gradients (Antoni *et al.*, 2016;
326 Takahashi *et al.*, 2002). Hydrotropism has been demonstrated to be independent of the auxin
327 induced gravitropism pathway and can compete in root angle changes against gravity (Dietrich
328 *et al.*, 2018). Based on the experiments presented here, we propose that the enhanced ABA flux
329 via the up-regulated NPF4 gene could be driving a low N-dependent shallow root angle change
330 while competing with the gravitropism pathway. As root angle is a determinant of root depth,
331 pursuing this gene function is of agronomic importance for improving foraging capacity and
332 uptake of nitrate in deep soil layers.

333

334 In summary, we found 55 root QTLs using a wheat seedling hydroponic system, 25 of which
335 were N-dependent. Using transcriptome analyses we found an up-regulated NPF family gene
336 likely transporting nitrate or ABA as part of an N-dependent response affecting root angle.
337 These findings provide a valuable genetic insight for root angle control, N-dependent responses
338 and candidate genes for improvement of N capture in wheat.

339 **Acknowledgements**

340 This work was supported by the Biotechnology and Biological Sciences Research Council
341 [grant number BB/M001806/1, BB/L026848/1, BB/P026834/1] (MJB, DMW, and MPP); the
342 Leverhulme Trust [grant number RPG-2016-409] (MJB and DMW); the European Research
343 Council FUTUREROOTS Advanced Investigator grant [grant number 294729] to MG, JAA,
344 DMW, and MJB; and the University of Nottingham Future Food Beacon of Excellence. The
345 authors would like to thank Limagrain UK Ltd for the use of the S×R DH population and Luzie
346 U. Wingen (John Innes Centre) for providing rQTL scripts used in this work.

Author Contribution

M.G. and J.A.A. performed the experiments with assistance from R.S. and D.M.W. The data was analysed by M.G., L.J.G. and M.H.W. The paper was written by M.G. and D.M.W. with input from all authors.

References

- Akpinar BA, Kantar M, Budak H. 2015.** Root precursors of microRNAs in wild emmer and modern wheats show major differences in response to drought stress. *Functional & Integrative Genomics* **15**, 587–598.
- An D, Su J, Liu Q, Zhu Y, Tong Y, Li J, Jing R, Li B, Li Z. 2006.** Mapping QTLs for nitrogen uptake in relation to the early growth of wheat (*Triticum aestivum* L.). *Plant and Soil* **284**, 73–84.
- Anders S, Huber W. 2010.** Differential expression analysis for sequence count data. *Genome biology* **11**, R106.
- Atkinson JA, Wingen LU, Griffiths M, Pound MP, Gaju O, Foulkes MJ, Le Gouis J, Griffiths S, Bennett MJ, King J, et al. 2015.** Phenotyping pipeline reveals major seedling root growth QTL in hexaploid wheat. *Journal of Experimental Botany* **66**, 2283–2292.
- Bai C, Liang Y, Hawkesford MJ. 2013.** Identification of QTLs associated with seedling root traits and their correlation with plant height in wheat. *Journal of Experimental Botany* **64**, 1745–1753.
- Beyer S, Daba S, Tyagi P, Bockelman H, Brown-Guedira G, Mohammadi M. 2018.** Loci and candidate genes controlling root traits in wheat seedlings—a wheat root GWAS. *Functional & Integrative Genomics*.
- Bolger AM, Lohse M, Usadel B. 2014.** Trimmomatic: a flexible trimmer for Illumina sequence data. *Bioinformatics* **30**, 2114–2120.
- Broman KW, Wu H, Sen S, Churchill GA. 2003.** R/qtl: QTL mapping in experimental crosses. *Bioinformatics* **19**, 889–890.
- Churchill GA, Doerge RW. 1994.** Empirical Threshold Values for Quantitative Trait Mapping. *Genetics* **138**, 963–971.
- Clark RT, Famoso AN, Zhao K, Shaff JE, Craft EJ, Bustamante CD, Mccouch SR, Aneshansley DJ, Kochian LV. 2013.** High-throughput two-dimensional root system phenotyping platform facilitates genetic analysis of root growth and development: Root phenotyping platform. *Plant, Cell & Environment* **36**, 454–466.
- Dawson J C, Huggins DR, Jones SS. 2008.** Characterizing nitrogen use efficiency in natural and agricultural ecosystems to improve the performance of cereal crops in low-input and organic agricultural systems. *Field Crops Research* **107**, 89–101.
- Delogu G, Cattivelli L, Pecchioni N, De Falcis D, Maggiore T, Stanca AM. 1998.** Uptake and agronomic efficiency of nitrogen in winter barley and winter wheat. *European Journal of Agronomy* **9**, 11–20.
- Edgar R C. 2004.** MUSCLE: multiple sequence alignment with high accuracy and high throughput. *Nucleic Acids Research*. **32**, 1792–1797.

El-Gebali S, Mistry J, Bateman A, Eddy SR, Luciani A, Potter SC, Qureshi M, Richardson LJ, Salazar GA, Smart A, et al. 2019. The Pfam protein families database in 2019. *Nucleic Acids Research* **47**, D427–D432.

Fang Z, Xia K, Yang X, Grotemeyer MS, Meier S, Rentsch D, Xu X, Zhang M. 2013. Altered expression of the PTR/NRT1 homologue OsPTR9 affects nitrogen utilization efficiency, growth and grain yield in rice. *Plant Biotechnology Journal* **11**, 446–458.

FAO. 2017. World fertilizer Trends and Outlook to 2020. Food and Agriculture Organization of the United Nations. Rome, Italy. Available online at: <http://www.fao.org/3/a-i6895e.pdf> (Accessed January 20, 2019).

Gelli M, Duo Y, Konda AR, Zhang C, Holding D, Dweikat I. 2014. Identification of differentially expressed genes between sorghum genotypes with contrasting nitrogen stress tolerance by genome-wide transcriptional profiling. *BMC genomics* **15**, 179.

Guo Y, Kong F, Xu Y, Zhao Y, Liang X, Wang Y, An D, Li S. 2012. QTL mapping for seedling traits in wheat grown under varying concentrations of N, P and K nutrients. *Theoretical and Applied Genetics* **124**, 851–865.

Habash DZ, Bernard S, Schondelmaier J, Weyen J, Quarrie SA. 2007. The genetics of nitrogen use in hexaploid wheat: N utilisation, development and yield. *Theoretical and Applied Genetics* **114**, 403–419.

Haley CS, Knott SA. 1992. A simple regression method for mapping quantitative trait loci in line crosses using flanking markers. *Heredity* **69**, 315–324.

Hodge A, Berta G, Doussan C, Merchan F, Crespi M. 2009. Plant root growth, architecture and function. *Plant and Soil* **321**, 153–187.

Huang N-C, Liu K-H, Lo H-J, Tsay Y-F. 1999. Cloning and Functional Characterization of an Arabidopsis Nitrate Transporter Gene That Encodes a Constitutive Component of Low-Affinity Uptake. *The Plant Cell* **11**, 1381–1392.

International Wheat Genome Sequencing Consortium. 2018. Shifting the limits in wheat research and breeding using a fully annotated reference genome. *Science* **361**, eaar7191.

Kanno Y, Hanada A, Chiba Y, Ichikawa T, Nakazawa M, Matsui M, Koshiba T, Kamiya Y, Seo M. 2012. Identification of an abscisic acid transporter by functional screening using the receptor complex as a sensor. *Proceedings of the National Academy of Sciences* **109**, 9653–9658.

Kant S, Bi Y-M, Rothstein SJ. 2010. Understanding plant response to nitrogen limitation for the improvement of crop nitrogen use efficiency. *Journal of Experimental Botany* **62**, 1499–1509.

Kawahara Y, de la Bastide M, Hamilton JP, Kanamori H, McCombie WR, Ouyang S, Schwartz DC, Tanaka T, Wu J, Zhou S, et al. 2013. Improvement of the *Oryza sativa* Nipponbare reference genome using next generation sequence and optical map data. *Rice* **6**, 4.

Krogh A, Larsson B, von Heijne G, Sonnhammer EL. 2001. Predicting transmembrane protein topology with a hidden markov model: application to complete genomes. *Journal of Molecular Biology* **305**, 567–580.

Krouk G, Crawford NM, Coruzzi GM, Tsay Y-F. 2010. Nitrate signaling: adaptation to fluctuating environments. *Current Opinion in Plant Biology* **13**, 265–272.

Landjeva S, Neumann K, Lohwasser U, Börner A. 2008. Molecular mapping of genomic regions associated with wheat seedling growth under osmotic stress. *Biologia Plantarum* **52**, 259–266.

Léran S, Varala K, Boyer J-C, Chiurazzi M, Crawford N, Daniel-Vedele F, David L, Dickstein R, Fernandez E, Forde B, *et al.* 2014. A unified nomenclature of NITRATE TRANSPORTER 1/PEPTIDE TRANSPORTER family members in plants. *Trends in Plant Science* **19**, 5–9.

Liu X, Li R, Chang X, Jing R. 2013. Mapping QTLs for seedling root traits in a doubled haploid wheat population under different water regimes. *Euphytica* **189**, 51–66.

Lobet G, Pound MP, Diener J, Pradal C, Draye X, Godin C, Javaux M, Leitner D, Meunier F, Nacry P, *et al.* 2015. Root System Markup Language: Toward a Unified Root Architecture Description Language. *Plant Physiology* **167**, 617–627.

Oono Y, Kawahara Y, Yazawa T, Kanamori H, Kuramata M, Yamagata H, Hosokawa S, Minami H, Ishikawa S, Wu J, *et al.* 2013. Diversity in the complexity of phosphate starvation transcriptomes among rice cultivars based on RNA-Seq profiles. *Plant Molecular Biology* **83**, 523–537.

Ouellette LA, Reid RW, Blanchard SG, Brouwer CR. 2018. LinkageMapView—rendering high-resolution linkage and QTL maps (O Stegle, Ed.). *Bioinformatics* **34**, 306–307.

Pertea M, Kim D, Pertea GM, Leek JT, Salzberg SL. 2016. Transcript-level expression analysis of RNA-seq experiments with HISAT, StringTie and Ballgown. *Nature Protocols* **11**, 1650–1667.

Pound MP, French AP, Atkinson JA, Wells DM, Bennett MJ, Pridmore T. 2013. RootNav: Navigating Images of Complex Root Architectures. *Plant Physiology* **162**, 1802–1814.

Reimand J, Arak T, Adler P, Kolberg L, Reisberg S, Peterson H, Vilo J. 2016. g:Profiler—a web server for functional interpretation of gene lists (2016 update). *Nucleic Acids Research* **44**, W83–W89.

Remans T, Nacry P, Pervent M, Filleur S, Diatloff E, Mounier E, Tillard P, Forde BG, Gojon A. 2006. The Arabidopsis NRT1. 1 transporter participates in the signaling pathway triggering root colonization of nitrate-rich patches. *Proceedings of the National Academy of Sciences* **103**, 19206–19211.

Ren Y, He X, Liu D, Li J, Zhao X, Li B, Tong Y, Zhang A, Li Z. 2012. Major quantitative trait loci for seminal root morphology of wheat seedlings. *Molecular Breeding* **30**, 139–148.

Schindelin J, Arganda-Carreras I, Frise E, Kaynig V, Longair M, Pietzsch T, Preibisch S, Rueden C, Saalfeld S, Schmid B, et al. 2012. Fiji: an open-source platform for biological-image analysis. *Nature Methods* **9**, 676–682.

Stamatakis A. 2014. RAxML version 8: a tool for phylogenetic analysis and post-analysis of large phylogenies. *Bioinformatics* **30**, 1312–1313.

Sun J, Guo Y, Zhang G, Gao M, Zhang G, Kong F, Zhao Y, Li S. 2013. QTL mapping for seedling traits under different nitrogen forms in wheat. *Euphytica* **191**, 317–331.

Wang J, Luo M-C, Chen Z, You FM, Wei Y, Zheng Y, Dvorak J. 2013. *Aegilops tauschii* single nucleotide polymorphisms shed light on the origins of wheat D-genome genetic diversity and pinpoint the geographic origin of hexaploid wheat. *New Phytologist* **198**, 925–937.

Yu P, Eggert K, von Wirén N, Li C, Hochholdinger F. 2015. Cell Type-Specific Gene Expression Analyses by RNA Sequencing Reveal Local High Nitrate-Triggered Lateral Root Initiation in Shoot-Borne Roots of Maize by Modulating Auxin-Related Cell Cycle Regulation. *Plant Physiology* **169**, 690–704.

Yu G, Smith DK, Zhu H, Guan Y, Lam TT-Y. 2017. ggtree: an r package for visualization and annotation of phylogenetic trees with their covariates and other associated data (G McInerney, Ed.). *Methods in Ecology and Evolution* **8**, 28–36.

Zhang H, Cui FA, Wang LIN, Li JUN, Ding A, Zhao C, Bao Y, Yang Q, Wang H. 2013. Conditional and unconditional QTL mapping of drought-tolerance-related traits of wheat seedling using two related RIL populations. *Journal of genetics* **92**, 213–231.

Zimin AV, Marçais G, Puiu D, Roberts M, Salzberg SL, Yorke JA. 2013. The MaSuRCA genome assembler. *Bioinformatics* **29**, 2669–2677.

Zurek PR, Topp CN, Benfey PN. 2015. Quantitative Trait Locus Mapping Reveals Regions of the Maize Genome Controlling Root System Architecture. *Plant Physiology* **167**, 1487–1496.

Table 1. Definition of plant traits measured.

Acronym	Definition	Software	Units
RTLA	Total length of all roots	RootNav	mm
RTLS	Total length of seminal roots	RootNav	mm
RTLL	Total length of lateral roots	RootNav	mm
RSC	Number of seminal roots	RootNav	Dimensionless (Count)
RLC	Number of lateral roots	RootNav	Dimensionless (Count)
RMW	Maximum width of the root system	RootNav	mm
RMD	Maximum depth of the root system	RootNav	mm
RWDR	Width-depth ratio (MW/MD)	RootNav	Dimensionless (Ratio)
RCMX	Root centre of mass- horizontal co-ordinate	RootNav	mm
RCMY	Root centre of mass - vertical co-ordinate	RootNav	mm
RCH	Convex hull - area of the smallest convex polygon to enclose the root system	RootNav	mm ²
RCHCX	Convex hull centroid - horizontal co-ordinate	RootNav	mm
RCHCY	Convex hull centroid - vertical co-ordinate	RootNav	mm
RAE1	Angle of emergence between the outermost seminal roots measured at 30 px	RootNav	Degrees (°)
RAE2	Angle of emergence between innermost pair of seminal roots measured at 30 px	RootNav	Degrees (°)
RAE951	Angle of emergence between outermost pair of seminal roots measured at 95 px	RootNav	Degrees (°)
RAE952	Angle of emergence between innermost pair of seminal roots measured at 95 px	RootNav	Degrees (°)
RAE251	Angle of emergence between outermost pair of seminal roots measured at first quartile of total length	RootNav	Degrees (°)
RAE252	Angle of emergence between innermost pair of seminal roots measured at first quartile of total length	RootNav	Degrees (°)
RAE501	Angle of emergence between outermost pair of seminal roots measured at second quartile of total length	RootNav	Degrees (°)
RAE502	Angle of emergence between innermost pair of seminal roots measured at first quartile of total length	RootNav	Degrees (°)
RAE751	Angle of emergence between outermost pair of seminal roots measured at third quartile of total length	RootNav	Degrees (°)
RAE752	Angle of emergence between innermost pair of seminal roots measured at third quartile of total length	RootNav	Degrees (°)
RAE1001	Angle of emergence between outermost pair of seminal roots measured at root tip	RootNav	Degrees (°)
RAE1002	Angle of emergence between innermost pair of seminal roots measured at root tip	RootNav	Degrees (°)
SH	Shoot height	FIJI	mm
SA	Shoot area	FIJI	mm ²

Table 2. Seedling phenotypic values for the S×R doubled haploid population and parents under two N regimes ($n = 18$, range = 8 to 36). Trait units as Table 1. Note: shoot data available for low N treatment only.

Trait	Treat	Savannah	Rialto	DH population			
		Mean ± SE	Mean ± SE	Mean ± SE	Range	Kurt	Skew
TLA	LN	536 ± 49	360.4 ± 24	485.7 ± 28	286.1 – 891	-0.5	0.5
	HN	668 ± 48	360 ± 28	479 ± 27	244 – 811	-0.5	0.3
TLS	LN	503 ± 39	353 ± 24	461 ± 24	280 – 791	-0.8	0.4
	HN	574 ± 32	345 ± 25	448 ± 23	240 – 651	-1	0
TLL	LN	33 ± 14	7.5 ± 2	25 ± 5	2.6 – 99	1.6	1.5
	HN	94.6 ± 23	15.4 ± 5	31.4 ± 6	1.5 – 176	7.1	2.3
RAE1	LN	85.7 ± 9	93.3 ± 6	92.4 ± 2	70 – 121	0.3	0.5
	HN	101 ± 10	103 ± 7	93.1 ± 4	56.7 – 140	0.3	0.4
RAE2	LN	49.1 ± 12	55.4 ± 6	60.5 ± 2	38.9 – 85	1.2	0.3
	HN	73.5 ± 6	62.8 ± 8	62.9 ± 2	39.7 – 95	0.3	0.5
LRC	LN	11.6 ± 7	4 ± 2	9.7 ± 1	1.7 – 28	0.6	1.2
	HN	20.9 ± 4	4.9 ± 1	9.1 ± 1	0.5 – 39	3.7	1.7
SRC	LN	4.7 ± 0.3	4.8 ± 0.1	4.6 ± 0.1	3.8 – 5	-0.1	-0.4
	HN	4.7 ± 0.2	5.2 ± 0.1	4.7 ± 0.1	3.8 – 5	0	-0.6
RCH	LN	11216 ± 2759	4540 ± 700	8893 ± 1015	2824 – 21774	-0.4	0.7
	HN	17832 ± 2498	4193 ± 792	9026 ± 950	2530 – 22836	-0.1	0.7
RMW	LN	108 ± 21	68.9 ± 7	94.3 ± 6	52.4 – 161	-0.7	0.5
	HN	138 ± 15	71.8 ± 7	89 ± 5	55.1 – 158	-0.2	0.7
RMD	LN	177 ± 15	113 ± 8	154 ± 8	94.7 – 240	-1.3	0.3
	HN	232 ± 15	118 ± 9	165 ± 8	89.5 – 246	-0.8	0
RWD	LN	0.6 ± 0.1	0.6 ± 0.1	0.6 ± 0	0.4 – 1	0.1	-0.2
	HN	0.6 ± 0.1	0.6 ± 0.1	0.6 ± 0	0.3 – 1	0.6	0.2
RCMX	LN	-0.9 ± 3	-3.4 ± 2	-2.7 ± 1	-14.2 – 2	3.3	-1.1
	HN	-2.3 ± 2	-0.5 ± 2	-1.9 ± 0	-9.6 – 1	0.9	-0.9
RCMY	LN	55.1 ± 4	36 ± 3	49.6 ± 3	29.2 – 73	-1.4	0.1
	HN	61.2 ± 3	30.6 ± 3	50.3 ± 3	23.5 – 73	-1	-0.2
RCHCX	LN	1.4 ± 5	-4.4 ± 2	-4.4 ± 1	-19.2 – 3	1.9	-0.9
	HN	-4.2 ± 5	-0.5 ± 2	-4.1 ± 1	-13.5 – 2	-0.6	-0.4
RCHCY	LN	85.3 ± 9	52.1 ± 4	74.2 ± 5	41.9 – 119	-1.3	0.3
	HN	103 ± 6	46.9 ± 4	76.2 ± 4	34.8 – 121	-0.9	0
RAE951	LN	81.4 ± 11	83.8 ± 6	82.2 ± 2	63.4 – 104	-0.1	0.1
	HN	95.9 ± 8	93.9 ± 6	87.9 ± 2	59.6 – 112	0	-0.3
RAE952	LN	46.7 ± 12	48.4 ± 5	51.9 ± 2	34.2 – 72	0	0
	HN	68.5 ± 9	54.4 ± 7	58.9 ± 2	35 – 88	0.4	0.2
RAE251	LN	76.8 ± 12	85.4 ± 6	78.5 ± 2	59.7 – 94	-0.5	-0.2
	HN	89.4 ± 7	92.2 ± 6	84 ± 2	60.2 – 104	-0.1	-0.2
RAE252	LN	50.4 ± 12	48.6 ± 5	49.1 ± 1	29.5 – 63	-0.4	-0.2
	HN	63.1 ± 8	55.9 ± 6	56.1 ± 2	36.8 – 83	0.1	0.3

RAE501	LN	71.8 ± 13	78.9 ± 6	73.2 ± 2	$53.8 - 90$	-0.2	0
	HN	87.9 ± 7	85.4 ± 7	79.4 ± 2	$59.3 - 99$	-0.1	-0.2
RAE502	LN	49.1 ± 10	47.5 ± 4	46.2 ± 1	$28.7 - 61$	-0.2	0
	HN	56.4 ± 9	54.8 ± 5	50.4 ± 2	$28.2 - 70$	-0.1	0
RAE751	LN	69.1 ± 12	74.7 ± 6	71.8 ± 2	$56.6 - 91$	0.2	0.3
	HN	87.2 ± 8	81.6 ± 7	76.7 ± 2	$55.6 - 96$	0	-0.1
RAE752	LN	50 ± 9	46 ± 4	46 ± 1	$30.4 - 59$	-0.2	0
	HN	53.7 ± 9	49.4 ± 6	47 ± 2	$26.6 - 63$	-0.3	-0.2
RAE1001	LN	68.6 ± 11	71.6 ± 6	71.3 ± 2	$55.7 - 92$	0.5	0.5
	HN	87.2 ± 8	76.5 ± 7	74.4 ± 2	$53.2 - 97$	0.4	0
RAE1002	LN	49.3 ± 8	43.8 ± 4	45.4 ± 1	$32 - 59$	-0.2	-0.1
	HN	51.8 ± 8	42.5 ± 6	43.5 ± 2	$21.4 - 59$	0.2	-0.4
SH	LN	72.4 ± 7	69.1 ± 3	75.8 ± 0	$51 - 90$	0.2	-0.4
SA	LN	137.9 ± 8	153.7 ± 5	165.8 ± 1	$85.4 - 271$	0.2	-0.4

Table 3. QTLs for wheat seedling traits detected in the S×R DH population grown in hydroponics. Trait units as Table 1. Note: shoot data available for low N treatment only.

Trait	Treat	QTL	Interval ^a	Site ^b		H2 ^c	
				(cM)	LOD ^c	Additive ^d	(%)
RTLA	LN	6D	BobWhite_c7090_522-BS00023964	5.0	27.4	-229	65.0
		7D	w SNP_Ku_c416_869895-BS00028760_51	26.0	8.4	-107	11.3
	HN	6D	BobWhite_c7090_522-BS00023964	4.4	23.0	-1275	57.4
		7D	w SNP_Ku_c416_869895-BS00028760_51	27.0	8.7	-703	14.3
RTLS	LN	6D	BobWhite_c7090_522-BS00023964	5.0	33.5	-198	70.5
		7D	w SNP_Ku_c416_869895-BS00028760_51	26.0	11.3	-86	12.1
	HN	6D	BobWhite_c7090_522-BS00023964	4.4	24.8	-1068	59.9
		7D	w SNP_Ku_c416_869895-BS00028760_51	27.0	9.4	-580	14.4
RTLL	LN	1A	BS00004043-BS00000226	215.0	2.3	-9.0	6.2
		6D	BobWhite_c7090_522-BS00023964	8.0	13.4	-31.2	48.0
	HN	6D	BS00009514-BS00023964	4.4	6.3	-208	28.0
RAE1	HN	3B	w SNP_RFL_Contig3336_3426054 GENE-1154_396-	178.8	2.2	-11.0	10.8
RAE2	HN	3B	w SNP_RFL_Contig3336_3426054	178.8	2.8	-8.2	13.3
RLC	LN	1A	BS00004043-BS00000226	216.0	4.9	-2.4	8.6
		6D	BobWhite_c7090_522-BS00023964	5.0	19.6	-9.4	52.8
		7D	w SNP_Ku_c416_869895-BS00028760_51	22.0	6.0	-4.4	10.9
	HN	6D	BS00009514-BS00023964	4.4	8.8	-8.5	36.5
RSC	LN	6D	BS00009514-BS00022787	4.4	3.2	0.2	13.1
		7D	w SNP_Ku_c416_869895-IAAV4624 Excalibur_c48636_283-	23.0	3.8	-0.2	15.8
	HN	7A	w SNP_RFL_Contig2864_2688208	12.0	2.9	0.2	13.7
RCH	LN	6D	BobWhite_c7090_522-BS00023964	4.4	31.1	-8464	80.0
		6D	BobWhite_c7090_522-BS00023964	4.4	18.4	-287837	53.5
	7D	w SNP_Ku_c416_869895-Kukri_c46303_512	34.0	4.2	-133799	8.3	
RMW	LN	1B	IAAV3905-w SNP_RFL_Contig3951_4390396	12.5	3.6	-8.9	5.0
		6D	BobWhite_c7090_522-BS00023964 w SNP_Ex_c9440_15657149-	4.4	26.7	-48.5	72.8
	HN	4D	w SNP_Ku_c16354_25219645	23.9	3.1	68.8	7.1
		6D	BS00009514-BS00023964	4.4	16.4	-230	54.6
RMD	LN	6D	BobWhite_c7090_522-BS00023964	4.4	31.5	-71.4	75.1
		7D	w SNP_Ku_c416_869895-BS00021859	27.0	3.7	-20.6	3.8
	HN	6D	BobWhite_c7090_522-BS00023964	4.4	21.8	-384	58.8
		7D	w SNP_Ku_c416_869895-BS00028760_51	30.0	5.2	-169	8.6
RMWD	HN	4D	w SNP_Ex_c9440_15657149-BS00065168	4.8	3.1	0.1	14.6
RCMX	LN	6D	BS00009514-BS00023964	6.0	2.3	1.6	11.2

	HN	1A	GENE-0249_122-BS00075532_51	145.0	4.1	-11.1	16.6
		6D	BS00009514-BS00023964	22.0	4.0	9.8	16.3
RCMY	LN	6D	BobWhite_c7090_522-BS00023964	4.4	31.9	-23.1	80.8
	HN	6D	BobWhite_c7090_522-BS00023964	4.4	19.5	-123	63.5
RCHCX	LN	6D	BS00009514-BS00023964	4.4	2.3	2.5	11.2
	HN	6D	BS00009514-BS00023964	18.0	3.2	13.6	12.9
		7D	wsnp_Ku_c416_869895-IAAV4624	21.0	3.2	16.5	13.1
RCHCY	LN	6D	BobWhite_c7090_522-BS00023964	4.4	34.1	-40.0	82.9
	HN	3B	BS00064778-BS00075879	216.2	4.9	45.2	6.8
		6D	BobWhite_c7090_522-BS00023964	4.4	25.0	-215.8	62.1
		7D	wsnp_Ku_c416_869895-Kukri_c46303_512 RAC875_c5799_224-	32.0	5.8	-91.8	8.2
RAE951	HN	3B	wsnp_Ra_c7158_12394405	178.8	2.8	-7.7	13.3
RAE251	LN	2D	BS00049876_51-BS00066132_51 BobWhite_c22370_352-	117.0	1.4	3.8	7.1
	HN	3B	wsnp_CAP11_c323_263800	178.8	3.6	-7.7	17.0
RAE252	HN	4D	wsnp_Ex_c9440_15657149-BS00065168	0.8	2.8	6.5	13.4
RAE501	HN	4D	wsnp_Ex_c9440_15657149-BS00065168	0.8	2.9	6.3	14.0
RAE502	HN	4D	wsnp_Ex_c9440_15657149-BS00065168	0.8	3.0	6.4	14.2
RAE751	LN	2D	BS00010393-BS00066132_51	160.0	2.6	5.1	12.5
	HN	4D	wsnp_Ex_c9440_15657149-BS00024014	0.8	2.9	6.3	13.8
RAE752	HN	4D	wsnp_Ex_c9440_15657149-BS00065168	0.8	2.1	5.3	10.4
RAE1001	LN	2D	BS00010393-BS00066132_51	160.0	3.0	5.5	14.3
	HN	4D	wsnp_Ex_c9440_15657149-BS00024014	0.8	2.4	6.0	11.9

^a Chromosome region of the QTL defined by two flanking markers

^b Genetic position of the QTL peak value

^c Logarithm of the odds value

^d Additive effects of putative QTL; a positive value indicates that positive alleles are from Savannah; negative values indicate positive alleles are from Rialto

^e Trait heritability

Table 4. Candidate genes for seminal root angle QTL located on chromosome 2D that were consistently expressed across the Group A replicates versus zero reads mapping in one or more Group B replicates. Gene naming convention according to IWGSC RefSeq v1.1.

Gene	Log ₂ fold change	p value	Functional annotation
TraesCS2D02G509700	1.73	0.002	Peroxidase
TraesCS2D02G344400	1.45	0.013	Unknown
MSTRG.42598 (TGACv1)	1.31	0.041	Unknown
TraesCS2D02G441300	1.29	0.037	AAA domain UvrD/REP helicase N-terminal domain
TraesCS2A02G111200	2.12	2.5E-05	Kelch motif
TraesCS2B02G126600	2.21	9.5E-06	Unknown
TraesCS2D02G487000	1.53	0.008	DUF wound-responsive family protein
TraesCS2D02G088100	1.29	0.036	C2H2-type zinc finger
TraesCS2D02G129100	1.36	0.036	Legume lectin domain
TraesCS2D02G330200	1.44	0.013	Unknown
MSTRG.40366 (TGACv1)	2.02	8.9E-05	Unknown
TraesCS2D02G108500	1.38	0.026	Peroxidase
TraesCS6A02G175000	1.66	0.002	Nuclear pore complex scaffold, nucleoporin
TraesCS2D02G270000	1.66	0.002	Helix-loop-helix DNA-binding domain
TraesCS2D02G511200	1.41	0.025	Peroxidase
TraesCS4B02G057100	1.48	0.013	Unknown
TraesCS2D02G348400	1.88	3.6E-04	NPF4